Commun. Comput. Phys.
doi: 10.4208/cicp.170414.231214a

Vol. **18**, No. 1, pp. 125-146
July 2015

Error Estimates of Some Numerical Atomic Orbitals in Molecular Simulations

Huajie Chen[1,*] and Reinhold Schneider[2]

[1] *Zentrum Mathematik, Technische Universität München, Boltzmannstraße 3, 85747 Garching, Germany.*
[2] *Institut für Mathematik, Technische Universität Berlin, Straße des 17. Juni 136, D-10623 Berlin, Germany.*

Communicated by Xingao Gong

Received 17 April 2014; Accepted (in revised version) 23 December 2014

Abstract. Numerical atomic orbitals have been successfully used in molecular simulations as a basis set, which provides a nature, physical description of the electronic states and is suitable for $\mathcal{O}(N)$ calculations based on the strictly localized property. This paper presents a numerical analysis for some simplified atomic orbitals, with polynomial-type and confined Hydrogen-like radial basis functions respectively. We give some a priori error estimates to understand why numerical atomic orbitals are computationally efficient in electronic structure calculations.

AMS subject classifications: 65N15, 65N25, 35P30, 81Q05

Key words: Kohn-Sham density functional theory, numerical atomic orbitals, Slater-type orbitals, a priori error estimate.

1 Introduction

In the *ab-initio* quantum mechanical modeling of many electron systems, Kohn-Sham density functional theory (KS-DFT) [28, 30] achieves so far the best compromise between accuracy and computational cost, and has become the most widely used electronic structure model in molecular simulations and materials science. Let us consider a closed-shell system with $M_{\rm n}$ nuclei of charges $\{Z_1,\cdots,Z_{M_{\rm n}}\}$, located at the positions $\{\mathbf{R}_1,\cdots,\mathbf{R}_{M_{\rm n}}\}$, and an even number $M_{\rm e}$ of electrons in the non-relativistic setting. The Kohn-Sham

*Corresponding author. *Email addresses:* chenh@ma.tum.de (H. Chen), schneidr@math.tu-berlin.de (R. Schneider)

 ©2015 Global-Science Press

https://doi.org/10.4208/cicp.170414.231214a Published online by Cambridge University Press

ground state energy and electron density of the system can be obtained by minimizing the energy functional

$$E\left[\{\phi_i\}_{i=1}^{M_e/2}\right]=\int_{\mathbb{R}^3}\left(\sum_{i=1}^{M_e/2}|\nabla\phi_i(\mathbf{r})|^2+v_{\text{ext}}(\mathbf{r})\rho(\mathbf{r})+e_{\text{xc}}[\rho(\mathbf{r})]\right)d\mathbf{r}$$
$$+\frac{1}{2}\int_{\mathbb{R}^3}\int_{\mathbb{R}^3}\frac{\rho(\mathbf{r})\rho(\mathbf{r}')}{|\mathbf{r}-\mathbf{r}'|}d\mathbf{r}d\mathbf{r}' \tag{1.1}$$

with respect to the orbitals $\{\phi_i\}_{i=1}^{M_e/2}$ under constraint $\int_{\mathbb{R}^3}\phi_i\phi_j=\delta_{ij}$, where

$$v_{\text{ext}}(\mathbf{r})=-\sum_{I=1}^{M_n}\frac{Z_I}{|\mathbf{r}-\mathbf{R}_I|} \tag{1.2}$$

is the electrostatic attraction potential generated by the nuclei, $\rho(\mathbf{r})=2\sum_{i=1}^{M_e/2}|\phi_i(\mathbf{r})|^2$ is the electron density, and $e_{\text{xc}}[\rho]$ is the exchange-correlation energy per volume with electron density ρ by a local density approximation (LDA, see [36]). The Euler-Lagrange equation associated with this minimization problem is the well-known Kohn-Sham equation: Find $\lambda_i\in\mathbb{R}$, $\phi_i\in H^1(\mathbb{R}^3)$ for $i=1,2,\cdots,M_e/2$, such that $\int_{\mathbb{R}^3}\phi_i\phi_j=\delta_{ij}$ and

$$\left(-\frac{1}{2}\Delta+v_{\text{eff}}[\rho]\right)\phi_i=\lambda_i\phi_i\quad\text{in }\mathbb{R}^3,\quad i=1,2,\cdots,M_e/2, \tag{1.3}$$

where $\{\lambda_i\}_{i=1}^{M_e/2}$ are the lowest $M_e/2$ eigenvalues, and $v_{\text{eff}}[\rho]=v_{\text{ext}}+v_{\text{H}}[\rho]+v_{\text{xc}}[\rho]$ is the effective potential with $v_{\text{H}}[\rho](\mathbf{r})=\int_{\mathbb{R}^3}\frac{\rho(\mathbf{r}')}{|\mathbf{r}-\mathbf{r}'|}d\mathbf{r}'$ being the Hartree potential for interactions between electrons and $v_{\text{xc}}[\rho]$ being the exchange-correlation potential [36]. A self-consistent field (SCF) iteration algorithm [33,36] is commonly resorted to for this nonlinear eigenvalue problem. In each iteration, a new Hamiltonian is constructed from a trial electronic state and a linear eigenvalue problem is then solved to obtain the low-lying eigenvalues. The algorithm requires expansions of the eigenfunctions by a finite set of simple known functions and discretization of the hamiltonian into a finite dimensional matrix. The choice of basis functions is therefore important, which ultimately determines the quality of the approximations.

Linear combination of atomic orbitals (LCAO) methods are the most widely used discretizations by chemists, which capture the essence of the atomic-like features and provide an intuitive description of electronic states. Generally, the atomic orbital basis functions are products of a radial basis function and a spherical harmonic function centered at each nuclear, that is

$$\psi_{Inlm}(\mathbf{r})=\chi_{Inl}(r_I)Y_{lm}(\hat{\mathbf{r}}_I),\quad I=1,\cdots,M_{\text{n}}, \tag{1.4}$$

where $\mathbf{r}_I=\mathbf{r}-\mathbf{R}_I$, $r=|\mathbf{r}|$, $\hat{\mathbf{r}}=\mathbf{r}/r$, and $Y_{lm}(\hat{\mathbf{r}})$ denotes the spherical harmonic functions on S^2. The radial basis functions χ_{Inl} depends on not only a site index I, but also an angular momentum quantum number l and a multiplicity index n. Among different basis

https://doi.org/10.4208/cicp.170414.231214a Published online by Cambridge University Press

functions, Gaussian-type orbitals (GTO) are used in the overwhelming majority of computations, which were first adopted by Boys [10] and then developed by many different approaches (see, e.g. [27,37,42]). The great virtue of GTO is that all matrix elements can be computed analytically, which simplifies and speeds up the calculations. Another group of analytically defined basis functions are Slater-type orbitals (STO), which capture the right behavior of electronic states both close to the nuclei and very far from them. For recent applications of DFT to chemically relevant problems, the numerical atomic orbitals (NAO) have been attracting much interest. The main feature of NAO is that the radial basis functions vanish over certain cutoff radii. Therefore, different spatial regions of large systems are strictly separated from one another, which can get rid of the troublesome introduced by long range terms and enable the $\mathcal{O}(N)$ methods for large scale electronic structure calculations [9,41]. We mention that great efforts have been made for developing $\mathcal{O}(N)$ methods of the eigenvalue problems (see, e.g. [23,33,36]), and most of these methods are formulated under an assumption that the basis functions are localized in real space. Therefore, the locality of the atomic orbitals can be fully utilized in large-scale DFT calculations coupled with $\mathcal{O}(N)$ methods.

Different ideas of constructing NAO basis functions have been proposed in the literature. Historically the first was the minimal confined free-atom-like excited state basis functions by [4]; further developments in [17,44] used the numerical orbitals obtained from direct solutions of the one-particle equations with free ions for a variable nuclear potential; [35] presented a systematic procedure to generate a basis set made of atomic orbitals and their derivatives with respect to the total electronic charge; [41] included polynomials in some given region to compensate the variational freedom; [39] constructed optimized numerical atomic orbitals ranging from element H to Kr, by taking the eigenstates, including excited states, of an atomic Kohn-Sham equation as primitive basis set, and then variationally optimizing the radial shape of numerical atomic orbitals within a cutoff radius. Moreover, many successfully used packages for quantum chemistry calculations are based on NAO basis functions, like SIESTA [41] and FHI-aims [9].

The main advantage of the atomic orbitals is their efficiency for molecular simulations (compared with other discretizations, the number of basis functions needed is usually much fewer for similar precision). The price to pay for this efficiency is the lack of systematic convergence. Unlike with plane-wave or real-space-grid related methods, there is no unique way of increasing the size of the basis set, and the rate of convergence depends on the way the basis set is enlarged. To our knowledge, there are only a handful of existing works devoted to the numerical analysis of atomic-like orbitals, see [5,31,32] for GTO approximations and [7,8] for exponential sum approximations, and there is no result dedicated to analysis of numerical atomic orbitals. The purpose of this paper is to provide an a priori error estimate for some typical numerical atomic orbitals.

First, we consider polynomial-type radial basis functions. By exploiting the theory of smooth partition of unity, the approximation errors can be estimated in each atomic sphere separately. A key point to the error estimate is the regularity of eigenfunctions in full-potential calculations. Since with the singular external potential given by (1.2),

https://doi.org/10.4208/cicp.170414.231214a Published online by Cambridge University Press

the eigenfunctions have cusps at the nuclear positions [22, 26], we can only obtain poor algebraic convergence rates that are far from satisfactory. Thanks to the recent studies in [19], which presents an asymptotically well behaved result for the eigenfunctions, we have higher regularities in weighted Sobolev space. It gives a better understanding of the singularity of the solution: indeed it appears that locally, when expressed in spherical coordinates around the nuclei, the solution is infinitely differentiable. This result is highly employed in our analysis and help us obtain spectral convergence rates.

Second, we consider the NAO basis functions with the radial part being eigenstates of hydrogen-like atoms in addition with an explicit confining potential. We point out that the space spanned by this type of basis functions is actually very close to that of STO. In our analysis, an a priori error estimate is given for STO basis functions, based on which the efficiency of the relative NAO is illustrated.

All results in this paper deal with the a priori error analysis. The a posteriori error analysis is even more difficult, which will be addressed in our forthcoming work. The remainder of this paper is arranged as follows. In the coming section, we present the model problem and some regularity results. In Section 3, we give the a priori error estimates for two types of numerical atomic orbitals with polynomial and hydrogen-like radial basis functions, respectively. Finally, we present some numerical experiments and future perspectives.

2 Preliminaries

We first introduce some notations. Let w be a certain weight function in a domain Ω, and $L^2_w(\Omega)$ be the weighted L^2 spaces, whose inner product and norm are given by

$$(u,v)_w = \int_\Omega w(\mathbf{r})u(\mathbf{r})v(\mathbf{r})d\mathbf{r}, \qquad \|u\|_{L^2_w(\Omega)} = \left(\int_\Omega u^2(\mathbf{r})w(\mathbf{r})d\mathbf{r}\right)^{1/2}.$$

The subscript w will be omitted from the notations in case of $w\equiv 1$. Throughout this paper, we shall denote by C a generic positive constant which stands for different values at its different occurrences. For convenience, the symbol $\lesssim$ will be used, and $A\lesssim B$ means that $A\leq CB$ for some constant C that is independent of discretization parameters. For $\mathbf{r}\in\mathbb{R}^3$, we shall denote by $r=|\mathbf{r}|$ and $\hat{\mathbf{r}}=\mathbf{r}/r$. Moreover, we shall denote $\sum_{l=0}^{\infty}\sum_{m=-l}^{l}$ by $\sum_{lm}^{\infty}$, and $\sum_{l=0}^{L}\sum_{m=-l}^{l}$ by $\sum_{lm}^{L}$ for summation of angular components.

Under the KS-DFT framework addressed in the introduction, the ground state solutions can be obtained by solving the Kohn-Sham equations (1.3). The weak form is

$$\begin{cases} \dfrac{1}{2}(\nabla\phi_i,\nabla\psi)+(v_{\text{eff}}[\rho]\phi_i,\psi)=\lambda_i(\phi_i,\psi) \quad \forall\,\psi\in H^1(\mathbb{R}^3), \quad i=1,2,\cdots,M_e/2, \\ \displaystyle\int_{\mathbb{R}^3}\phi_i\phi_j=\delta_{ij}, \end{cases} \tag{2.1}$$

where the electron density ρ and effective potential $v_{\text{eff}}[\rho]$ are given as that in (1.3), and the lowest $M_e/2$ eigenvalues are to be solved. Since ρ is given by eigenfunctions

https://doi.org/10.4208/cicp.170414.231214a Published online by Cambridge University Press

$\{\phi_i\}_{i=1}^{M_e/2}$, (2.1) is a nonlinear eigenvalue problem, which is usually solved by SCF algorithms. With a trial electron density $\tilde{\rho}$, we substitute $v_{\text{eff}}[\rho]$ by $v_{\text{eff}}[\tilde{\rho}]$ and solve a linear eigenvalue problem at each step of the iterations.

Denote $v_{\text{eff}}[\tilde{\rho}]$ by v_{eff} for convenience, we have the following Schrödinger-type linear eigenvalue problem: Find $\lambda\in\mathbb{R}$ and $0\neq u\in H^1(\mathbb{R}^3)$ such that $\|u\|_{L^2(\mathbb{R}^3)=1}$ and

$$a(u,v)=\lambda(u,v)\quad\forall\, v\in H^1(\mathbb{R}^3), \tag{2.2}$$

where the bilinear form $a(\cdot,\cdot):H^1(\mathbb{R}^3)\times H^1(\mathbb{R}^3)\to\mathbb{R}$ is defined by

$$a(u,v)=\frac{1}{2}\int_{\mathbb{R}^3}\nabla u\cdot\nabla v+\int_{\mathbb{R}^3}v_{\text{eff}}uv. \tag{2.3}$$

Note that the effective potential v_{eff} is not smooth due to the singularities of v_{ext} at nuclear positions $\mathbf{R}_I$ $(I=1,\cdots,M_n)$.

A nature and important question is what the regularity of the eigenfunctions is. We shall present some regularity results in the rest part of this section, which is crucial to our analysis. For simplicity of presentations, we will temporarily focus ourselves on the linearized problem (2.2) and assume $M_n=1$ with $\mathbf{R}_1=(0,0,0)$, that is, the system has only one nucleus located at the origin. Note that for systems with arbitrary number of nuclei, all the following discussions can be carried out for each nucleus separately.

It is shown (see, e.g. [20–22,24,26]) that the exact eigenfunctions of such problems are analytic away from the nuclei, and satisfy certain cusp conditions at the nuclear positions (the regularity is not better than $H^{5/2}$ around the singularities). In our analysis, we rely on the regularity results in weighted Sobolev spaces developed in [19]. This type of analysis has been introduced to investigate singularities of boundary value problems in conical domains with corners and edges, see [6,11,18] for further details. In our case, the geometry is fairly simple, but the singular electrostatic potential generated by nuclei still fits perfectly into this framework.

We define the space

$$H^k_{\text{cone}}(\mathbb{R}^3)=\{u\in H^k_{\text{loc}}(\mathbb{R}\times S^2)|_{\mathbb{R}_+\times S^2}:(1-\omega)u\in H^k(\mathbb{R}^3)\}, \tag{2.4}$$

where ω is a smooth cutoff function, that is, $\omega=1$ near the origin and $\omega=0$ outside some neighborhood of zero. Further, we define the kth weighted Sobolev space with index γ by

$$\mathcal{K}^{k,\gamma}(\mathbb{R}^3)=\left\{u(\mathbf{r})\in L^2(\mathbb{R}^3)\,:\,r^{|\alpha|-\gamma}\partial^\alpha u\in L^2(\mathbb{R}^3)\ \ \forall\,|\alpha|\leq k\right\}, \tag{2.5}$$

where $k\in\mathbb{N}$ and $\gamma\in\mathbb{R}$. The difference between the spaces $H^k(\mathbb{R}^3)$ and $\mathcal{K}^{k,\gamma}(\mathbb{R}^3)$ only lies in the introduction of the weight functions $r^{|\alpha|-\gamma}$. Note that neither (2.4) nor (2.5) is really appropriate for our purposes. Instead, we consider the combination

$$\mathcal{K}^{k,\gamma}_{\text{cone}}(\mathbb{R}^3):=\omega\mathcal{K}^{k,\gamma}(\mathbb{R}^3)+(1-\omega)H^k_{\text{cone}}(\mathbb{R}^3), \tag{2.6}$$

https://doi.org/10.4208/cicp.170414.231214a Published online by Cambridge University Press

which provides the appropriate behavior at the limits $|\mathbf{r}|\to 0$ and $|\mathbf{r}|\to\infty$ simultaneously. We now consider subspaces $\mathscr{K}^{k,\gamma}(\mathbb{R}^3)$ of $\mathcal{K}^{k,\gamma}_{\text{cone}}(\mathbb{R}^3)$, defined by

$$\mathscr{K}^{k,\gamma}(\mathbb{R}^3)=\Big\{u\in\mathcal{K}^{k,\gamma}_{\text{cone}}(\mathbb{R}^3):u(\mathbf{r})-\omega(\mathbf{r})\sum_{j=0}^{n}c_j(\hat{\mathbf{r}})r^j\in\mathcal{K}^{k,\gamma+n}_{\text{cone}}(\mathbb{R}^3),\ \forall\, n\in\mathbb{N}\Big\}. \tag{2.7}$$

Here each c_j belongs to the finite dimensional subspace $M_j=\text{span}\{Y_{lm},0\le l\le j,|m|\le l\}\subset C^\infty(S^2)$ and Y_{lm} denotes the spherical harmonic function on S^2. On a more intuitive level, this means that these spaces consist of functions with asymptotic expansions of the type

$$u(\mathbf{r})\sim\sum_{j\in\mathbb{N}_0}c_j(\hat{\mathbf{r}})r^j\quad\text{as}\ \ r\to 0, \tag{2.8}$$

where the powers of r can only be nonnegative integers, and the corresponding remainders belong to higher order weighted Sobolev spaces. We shall use such weighted Sobolev spaces with asymptotic type (2.8) within a particular range of parameters γ, which motivates the following definition.

Definition 2.1. A function u is called *asymptotically well behaved* if $u\in\mathscr{K}^{\infty,\gamma}(\Omega)$ for $\gamma<3/2$.

For the regularity results of this section, we make the assumption that the effective potential in (2.3) is of the form

$$v_{\text{eff}}(\mathbf{r})=-\frac{Z}{|\mathbf{r}|}+\tilde{\rho}*\frac{1}{|\mathbf{r}|}+v_{\text{s}}(\mathbf{r}), \tag{2.9}$$

where v_{s} and the trial electron density $\tilde{\rho}$ are assumed to be asymptotically well behaved functions. The following proposition gives the regularity result for eigenfunctions of (2.2).

Proposition 2.1. If u is an eigenfunction of (2.2) with potential of the form (2.9), then u is asymptotically well behaved.

When v_{s} is the exchange potential in the Hartree-Fock model, the proof of the above proposition is provided in [19, Theorem 1]; for other cases that correspond to the linearized Kohn-Sham equations (including hybrid functionals), one can follow the lines of this proof to obtain the result in an analogous manner.

Remark 2.1. For nonlinear Kohn-Sham equations (2.1) with usual LDA, we note that the assumption of such v_s being asymptotically well behaved is not known to our knowledge due to the singularities of exchange-correlation potentials used in practice. As a consequence, the above regularity result may not be directly applied to Kohn-Sham equations in the LDA setting. A further investigation of different density functionals concerning this condition is beyond the scope of this work.

https://doi.org/10.4208/cicp.170414.231214a Published online by Cambridge University Press

Denote by $\mathcal{Y}_{lm}$ the solid harmonic function

$$\mathcal{Y}_{lm}(\mathbf{r}) = r^l Y_{lm}(\hat{\mathbf{r}}).$$

Since $\mathcal{Y}_{lm}(\mathbf{r})$ has explicit Cartesian expressions (see, e.g. [27]) as

$$\begin{aligned}\mathcal{Y}_{lm}(\mathbf{r}) &= \mathcal{Y}_{lm}(\mathbf{r}(x,y,z)) = \mathcal{P}_{lm}(x,y,z)\\ &= N_{lm}(x+\mathrm{sgn}(m)iy)^{|m|}\sum_{t=0}^{(l-|m|)/2} C_t^{l|m|}(x^2+y^2)^t z^{l-2t-|m|}\end{aligned} \tag{2.10}$$

with the constants N_{lm} and $C_t^{l|m|}$, it yields a significant simplification for numerical integrations in computations (see [27]). Therefore, the solid harmonic functions are always used as the angular parts of the atomic bases instead of spherical harmonics $Y_{lm}(\hat{\mathbf{r}})$. The following proposition will be used in our analysis, the proof of which is given in [5, Proposition 2].

Proposition 2.2. If u is an eigenfunction of (2.2) with potential of the form (2.9), then

$$u \in C^\infty(\overline{\mathbb{R}}_+ \times S^2), \tag{2.11}$$

and it can be expanded by solid harmonics as

$$u(\mathbf{r}) = \sum_{lm}^{\infty} R_{lm}(r)\mathcal{Y}_{lm}(\mathbf{r}) \tag{2.12}$$

with $R_{lm} \in C^\infty(\overline{\mathbb{R}}_+)$.

Beside the regularities near the nuclear positions, we shall also need the behavior of eigenfunctions far away from them. It is known that under certain restrictions on v_{eff}, the eigenfunctions of (2.2) decay exponentially fast to 0 as $r \to \infty$ (see, e.g. [2,43]), i.e., the functions

$$\mathbf{r} \to u(\mathbf{r})e^{-\alpha r}, \quad (\nabla u)(\mathbf{r})e^{-\beta r} \tag{2.13}$$

are square integrable with some constants α and β. This exponential decay property can be proven for the electronic Schrödinger equation [26,43], for the Hartree-Fock equations [34], and also for some Kohn-Sham equations [1,3].

3 Analysis of two numerical atomic orbitals

In this section, we shall give a numerical analysis for two types of numerical atomic orbitals. Let V_δ be the finite dimensional space spanned by the NAO basis functions $\{\psi_\mu\}_{1\le\mu\le N_\delta}$. The solution to the Galerkin approximation is given by

$$u_\delta(\mathbf{r}) = \sum_{\mu=1}^{N_\delta} C_\mu \psi_\mu(\mathbf{r}),$$

https://doi.org/10.4208/cicp.170414.231214a Published online by Cambridge University Press

and the variational approximation of (2.2) is

$$a(u_\delta,v)=\lambda_\delta(u_\delta,v) \quad \forall\, v\in V_\delta. \tag{3.1}$$

This is equivalent to a generalized eigenvalue problem

$$HC=\lambda_\delta SC,$$

where the Hamilton matrix H and overlap matrix S are determined by the following integrations

$$H_{ij}=\int_{\mathbb{R}^3}\big(\frac{1}{2}\nabla\psi_i(\mathbf{r})\nabla\psi_j(\mathbf{r})+v_{\text{eff}}(\mathbf{r})\psi_i(\mathbf{r})\psi_j(\mathbf{r})\big)d\mathbf{r}, \qquad S_{ij}=\int_{\mathbb{R}^3}\psi_i(\mathbf{r})\psi_j(\mathbf{r})d\mathbf{r}. \tag{3.2}$$

Using the standard estimates [38, 43], we have that the H^1-norm error of the finite dimensional approximation is estimated by

$$\|u-u_\delta\|_{H^1(\mathbb{R}^3)}\leq C\inf_{v_\delta\in V_\delta}\|u-v_\delta\|_{H^1(\mathbb{R}^3)}. \tag{3.3}$$

For nonlinear Kohn-Sham equation (2.1), we have the following discrete problem

$$\begin{cases}\dfrac{1}{2}\big(\nabla\phi_{i,\delta},\nabla v\big)+\big(v_{\text{eff}}[\rho_\delta]\phi_{i,\delta},v\big)=\lambda_{i,\delta}\big(\phi_{i,\delta},v\big) \quad \forall\, v\in V_\delta, \quad i=1,2,\cdots,M_{\text{e}}/2,\\ \displaystyle\int_{\mathbb{R}^3}\phi_{i,\delta}\phi_{j,\delta}=\delta_{ij},\end{cases}$$

with $\rho_\delta(\mathbf{r})=2\sum_{i=1}^{M_{\text{e}}/2}|\phi_{i,\delta}(\mathbf{r})|^2$. Using the same arguments as those in [14] (see also [12]), we can obtain the following estimate under certain assumptions (we need the coercivity assumption on the tangent space, the regularity assumption of the exchange-correlation term e_{xc}, and the completeness assumption of the limit of the finite dimensional space, see [12, 14])

$$\sum_{i=1}^{M_{\text{e}}/2}\|\phi_i-\phi_{i,\delta}\|_{H^1(\mathbb{R}^3)}\lesssim\sup_{1\leq i\leq M_{\text{e}}/2}\inf_{v_\delta\in V_\delta}\|\phi_i-v_\delta\|_{H^1(\mathbb{R}^3)}. \tag{3.4}$$

Note that the convergence rate of ground state energy approximation is quadratic to that of H^1-norm [12, 15], i.e.

$$|E-E_\delta|\lesssim\sum_{i=1}^{M_{\text{e}}/2}\|\phi_i-\phi_{i,\delta}\|^2_{H^1(\mathbb{R}^3)},$$

which implies that an H^1-error estimate is of most interest and in some sense sufficient. Therefore it is only necessary for us to obtain the estimates for the right hand side of (3.3) and (3.4) with a specified V_δ.

https://doi.org/10.4208/cicp.170414.231214a Published online by Cambridge University Press

As formulated in the introduction, the NAO basis functions are products of numerical radial functions and spherical harmonics centered at nuclear positions,

$$\psi_{Inlm}(\mathbf{r}) = \chi_{Inl}(r_I)Y_{lm}(\hat{\mathbf{r}}_I) \tag{3.5}$$

with $\mathbf{r}_I = \mathbf{r} - \mathbf{R}_I$. In contrast to the STO and GTO basis functions, the radial basis function χ_{Inl} for NAO is strictly localized inside a given cutoff radius R_I^{cut} for each nucleus and angular momentum, i.e.,

$$\psi_{Inlm}(\mathbf{r}) = 0 \quad \text{if } r_I \geq R_I^{\text{cut}}. \tag{3.6}$$

Here, for simplicity of analysis, we assume that the cutoff radii are independent of the angular momentum l. Thanks to the locality property (3.6), different spatial regions of large systems are thus strictly separated from one another, which gets rid of the troublesome introduced by long range terms and enable the $\mathcal{O}(N)$ methods for large scale electronic structure calculations [9, 41]. Generally, in the DFT calculations using NAO, the computational accuracy and efficiency can be controlled by two simple parameters: the cutoff radii and the number of orbitals per atom.

To construct the basis functions (3.5), we shall first partition the domain into overlapping atom-centered spheres $\Omega_I = B(\mathbf{R}_I, R_I^{\text{cut}})$ with R_I^{cut} sufficiently large so that there is no interstitial region between the atoms (see Fig. 1). We mention that our theory also allows to include (ghost) spheres that are not centered at any atom [36, 41], which are helpful for filling the space and calculating the counterpoise corrections for superposition errors. Moreover, we need a Ω_0 to denote the rest part of $\mathbb{R}^3$, i.e.

$$\Omega_0 = \mathbb{R}^3 \setminus \left(\bigcup_{I=1}^{M_{\text{n}}} B(\mathbf{R}_I, R_I^{\text{cut}} - \varepsilon) \right)$$

with $\varepsilon > 0$, so that $\mathbb{R}^3 = \bigcup_{I=0}^{M_{\text{n}}} \Omega_I$.

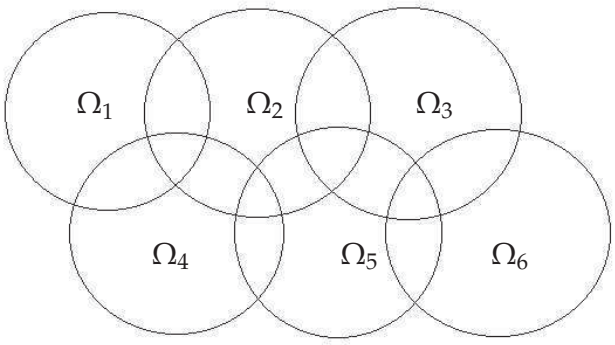


Figure 1: The partition of the domain into atomic spheres.

https://doi.org/10.4208/cicp.170414.231214a Published online by Cambridge University Press

With the above partition, we can construct localized atomic orbitals in each Ω_I $(1\leq I\leq M_{\rm n})$. Generally, a set of atomic orbitals shall be generated by simple parameters as few as possible, which means that the basis functions are systematically available as many as we want. A simple and mathematically intuitive choice is to take χ_{Inl} by polynomials with order less or equal to n. We mention that although this type of basis functions are not used alone due to the difficulties in numerical implementations, they are still partially included to compensate the variational freedoms in practice (see [41]). Another way to generate χ_{Inl} is to take numerical solutions of the one-particle Schrödinger-like equations with variable nuclear potential together with a confining potential. We shall present some numerical analysis for both of these constructions in the rest part of this section.

First, we need some regularity assumptions for the eigenfunctions based on the partition $\{\Omega_I\}_{0\leq I\leq M_{\rm n}}$. Let $\omega_0\equiv 0$, and $\omega_I\geq 0$ $(1\leq I\leq M_{\rm n})$ be the smooth cutoff functions, such that ω_I equals 1 at the neighbor of $\mathbf{R}_I$ and vanish in any other $\Omega_{I'}$ with $I'\neq I$. It is obvious that $\sum_{I=1}^{M_{\rm n}}\omega_I(\mathbf{r})\leq 1\ \forall\ \mathbf{r}\in\mathbb{R}^3$. Let

$$\Omega=\bigcup_{I=1}^{M_{\rm n}}\Omega_I \qquad \text{and} \qquad f=1-\sum_{I=1}^{M_{\rm n}}\omega_I(\mathbf{r}).$$

Note that f is a smooth function on $\mathbb{R}^3$ and vanishes at the neighbor of $\mathbf{R}_I$ $(I=1,\cdots,M_{\rm n})$. Using the partition of unity theory and the fact that Ω_Is are overlapping, we have that there exist smooth functions f_I $(I=0,\cdots,M_{\rm n})$, such that $\text{supp}\{f_I\}\subset\Omega_I$ and $f=\sum_{I=0}^{M_{\rm n}}f_I$. Let

$$u_I=(\omega_I+f_I)u,$$

we have

1. $\text{supp}\{u_I\}\subset\Omega_I$;
2. $u_I=u$ in the neighborhood of $\mathbf{R}_I$;
3. $\sum_{I=0}^{M_{\rm n}}u_I=u$.

By the above properties of u_I and Proposition 2.2, we can write u_I as

$$u_I(\mathbf{r}_I)=\sum_{lm}^{\infty}R_{Ilm}(r_I)\mathcal{Y}_{lm}(\mathbf{r}_I)$$

with $\mathbf{r}_I=\mathbf{r}-\mathbf{R}_I$ and $R_{Ilm}\in C^\infty([0,R_I^{\rm cut}])$. Let $\hat{\partial}=\partial+\frac{1}{2}$, we make the following assumptions based on the regularity results in Section 2:

A. $\sum_{I=1}^{M_{\rm n}}\|u_I\|_{H^s([0,R_I^{\rm cut}]\times S^2)}<\infty$ for any $s\in\mathbb{R}^+$;

https://doi.org/10.4208/cicp.170414.231214a Published online by Cambridge University Press

B. $\sum_{I=1}^{M_n}\sum_{lm}^{\infty}\|\hat{\partial}^s R_{Ilm}\|_{L^2_{r^{2l+s}}([0,R_I^{cut}])}<\infty$ for any $s\in\mathbb{R}^+$;

C. $\|u\|_{H^1(\Omega_0)}\leq ce^{-\alpha R}$ with α being some constant and R being radius of the biggest ball contained in Ω.

Here $[0,R_I^{cut}]\times S^2$ in **A** and **B** is nothing but an spherical coordinate representation of the atomic sphere Ω_I centered at $\mathbf{R}_I$.

Assumption **A** is true by applying (2.11) to each u_I around $\mathbf{R}_I$ separately. Assumption **B** is a quite restrictive additional condition, which requires fast decay of $\|R_{Ilm}\|_{H^s([0,R_I^{cut}])}$ with respect to angular number l. Although Proposition 2.2 indicates that $\|R_{Ilm}\|_{H^s([0,R_I^{cut}])}$ is finite for each I, l and m, it is still not sufficient to ensure the summation in **B**. We can not prove **B** if there are infinite angular components of u_I, and **B** will not be used for all our estimates. Fortunately, it is observed from the numerical tests (e.g. [9]) that omitting high angular momentum functions (like g, h functions) from the basis sets does not significantly affect the results. In fact, most of the numerical simulations with NAO use high angular momentums up to g function (i.e. $l\leq 4$). This means that our assumption in **B** is reasonable and make sense in practice. Assumption **C** is nothing but a reformulation of the exponential decay result (2.13).

3.1 Polynomial-type atomic orbitals

Consider the simple polynomial-type radial basis functions

$$\chi_{Inl}(r)=c_n(r-R_I^{cut})^n,\qquad n=1,2,\cdots \tag{3.7}$$

with c_n being the normalization constants. Note that χ_{Inl} in (3.7) does not depend on the angular number l. The corresponding finite dimensional space is

$$\begin{aligned}V_\delta\equiv V_{NL}=\mathrm{span}\big\{&c_n(r_I-R_I^{cut})^nY_{lm}(\hat{\mathbf{r}}_I):\\ &1\leq I\leq M_n,\,1\leq n\leq N,\,0\leq l\leq L,\,|m|\leq l\big\}.\end{aligned} \tag{3.8}$$

The following lemma will be used (see [5, 15] for its proof), which states the relationship between two Sobolev norms.

Lemma 3.1. *If $v\in H^1(B(\mathbf{0},R))\bigcap H^1([0,R]\times S^2)$, then there exists a constant C such that*

$$\|v\|_{H^1(B(\mathbf{0},R))}\leq C\|v\|_{H^1([0,R]\times S^2)}.$$

Theorem 3.1. *Let V_δ be given by* (3.8). *If u satisfies the assumptions* **A** *and* **C**, *then for any $s>1$ we have*

$$\inf_{v_\delta\in V_\delta}\|u-v_\delta\|_{H^1(\mathbb{R}^3)}\leq C_s(L^{-(s-1)}+N^{-(s-1)})+Ce^{-\alpha R}, \tag{3.9}$$

where C_s is a constant depending on u and s only.

https://doi.org/10.4208/cicp.170414.231214a Published online by Cambridge University Press

Proof. For any $V_\delta \ni v_\delta = \sum_{I=1}^{M_n} v_{\delta,I}$ with $v_{\delta,I}$ spanned by the basis functions centered at $\mathbf{R}_I$, we have

$$\begin{aligned}\|u-v_\delta\|_{H^1(\mathbb{R}^3)} &= \|\sum_{I=0}^{M_n} u_I - v_\delta\|_{H^1(\mathbb{R}^3)} \\ \leq \|f_0 u\|_{H^1(\Omega_0)} + \|\sum_{I=1}^{M_n}(u_I - v_{\delta,I})\|_{H^1(\cup_{I=1}^{M_n}\Omega_I)} &\leq Ce^{-\alpha R} + \sum_{I=1}^{M_n}\|u_I - v_{\delta,I}\|_{H^1(\Omega_I)}, \end{aligned} \tag{3.10}$$

where the assumption **C** is used for the last inequality. For approximation of u_I, we define the projection operators $P_{N,I}: H^1([0,R]) \to \Psi_N = \text{span}\{c_n(r-R_I^{\text{cut}})^n, 1\leq n\leq N\}$ satisfying

$$(\nabla(v-P_{N,I}v), \nabla\psi) = 0 \quad \forall\, \psi \in H^1([0,R])$$

and $P_L: L^2(S^2) \to M_L = \text{span}\{Y_{lm}, 0\leq l\leq L, |m|\leq l\}$ by

$$P_L\varphi(\hat{\mathbf{r}}) = \sum_{lm}^{L} \check{\varphi}_{lm} Y_{lm}(\hat{\mathbf{r}}) \quad \text{with} \quad \check{\varphi}_{lm} = \int_{S^2} \varphi(\hat{\mathbf{r}}) Y_{lm}(\hat{\mathbf{r}}) d\hat{\mathbf{r}}.$$

Define the projection operator $\mathbb{P}^{NL,I}: H^1([0,R_I^{\text{cut}}]\times S^2) \to \Psi_N \times M_L$ by $\mathbb{P}^{NL,I} = P_{N,I} \circ P_L$. Using standard error estimates for polynomial and spherical harmonic approximations, we obtain that for any $u_I \in H_0^1(B(\mathbf{R}_I, R_I^{\text{cut}})) \cap H^s([0,R_I^{\text{cut}}]\times S^2)$,

$$\|u_I - \mathbb{P}^{NL,I}u_I\|_{H^1([0,R_I^{\text{cut}}]\times S^2)} \leq C(L^{-(s-1)} + N^{-(s-1)})\|u_I\|_{H^s([0,R_I^{\text{cut}}]\times S^2)} \quad \forall\, s>1. \tag{3.11}$$

By taking $v_{\delta,I} = \mathbb{P}^{NL,I}u_I$, we have from Lemma 3.1 and (3.11) that

$$\begin{aligned}\|u_I - v_{\delta,I}\|_{H^1(\Omega_I)} &\leq \|u_I - v_{\delta,I}\|_{H^1([0,R_I^{\text{cut}}]\times S^2)} \\ &\leq C(L^{-(s-1)} + N^{-(s-1)})\|u_I\|_{H^s([0,R_I^{\text{cut}}]\times S^2)} \quad \forall\, s>1. \end{aligned} \tag{3.12}$$

Then we can obtain (3.9) from (3.10), (3.12) and the assumption **A**, which completes the proof. □

It is shown by Theorem 3.1 that the computational accuracy can be controlled by two simple parameters: the cutoff radii and the number of atomic orbitals. If the cutoff radii are sufficiently large, then we have a super-algebraic convergence rate for approximation errors.

3.2 Confined Hydrogen-like atomic orbitals

In many NAO based molecular simulations, localized orbitals (3.5) are constructed from atomic-like programs with spherically symmetric potentials (e.g. [9, 36, 39, 41]). More

https://doi.org/10.4208/cicp.170414.231214a Published online by Cambridge University Press

specifically, the radial basis χ_{Inl} are numerical solutions of the following eigenvalue problem

$$\left(-\frac{1}{2}\frac{d^2}{dr^2}+\frac{l(l+1)}{2r^2}+v_{In}(r)\right)(r\chi_{Inl}(r))=\lambda_n(r\chi_{Inl}(r)), \tag{3.13}$$

where the radial potential v_{In} is

$$v_{In}(r)=-\frac{Z_{In}}{r}+v_I^{\text{conf}}(r) \tag{3.14}$$

in full-potential calculations. The first part of (3.14) defines the main behavior of the eigenfunctions. One possible choice of Z_{In} is to take a fixed number for each I, however, the efficiency of this kind of basis set is rather low. Thus, the eigenfunctions of different ionization states are used in practice. The second part v_I^{conf} is a steeply increasing confining potential that ensures χ_{Inl} to smoothly decay to zero at the cutoff radius R_I^{cut}. Fig. 2 gives a schematic plot of the confining potential, which is 0 in most parts of the atomic spheres and increase smoothly to ∞ near R_I^{cut}.

Remark 3.1. Note that in many calculations, the radial basis functions are required to be continuous up to the third derivatives around the cutoff radii (so that matrix elements for the kinetic operator are continuous up to the first derivatives to realize a stable geometry optimization and molecular dynamics simulations). Therefore, the confining potential shall be smooth enough to make χ_{Inl} suited. One proposal of v_I^{conf} is [9]

$$v_I^{\text{conf}}(r)=\begin{cases}0, & r\le R_I^{\text{set}},\\ \dfrac{c}{(r-R_I^{\text{cut}})^2}\exp\left(\dfrac{1}{R_I^{\text{set}}-r}\right), & R_I^{\text{set}}<r<R_I^{\text{cut}},\\ \infty, & r\ge R_I^{\text{cut}},\end{cases} \tag{3.15}$$

with some constant c and $R_I^{\text{set}}\in(0,R_I^{\text{cut}})$.

We are not able to give the a priori error estimate for the basis functions given by (3.13) due to the various choices of Z_{In} and v_I^{conf}. Instead, we consider the eigenfunctions of

$$\left(-\frac{1}{2}\frac{d^2}{dr^2}+\frac{l(l+1)}{2r^2}-\frac{Z_{In}}{r}\right)(r\tilde{\chi}_{Inl}(r))=\lambda_n(r\tilde{\chi}_{Inl}(r)), \tag{3.16}$$

that is, the equation without confining potential v_I^{conf}. Note that the main behavior of χ_{Inl} is defined by potential $-Z_{In}/r$, and the effect of v_I^{conf} is only to make χ_{Inl} smoothly decay to 0 around R_I^{cut}. Since the eigenfunctions of (3.16) decay to 0 exponentially fast with respect to r, we can say that χ_{Inl} and $\tilde{\chi}_{Inl}$ are highly related to each other (see Fig. 3 for a comparison with $Z_{In}=n$ in the following).

https://doi.org/10.4208/cicp.170414.231214a Published online by Cambridge University Press

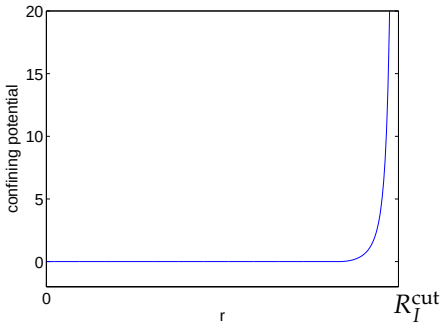


Figure 2: A schematic plot of the confining potential.

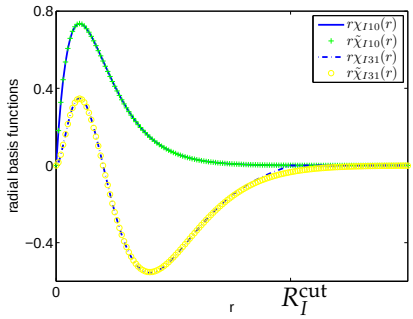


Figure 3: Comparison of χ_{Inl} and $\tilde{\chi}_{Inl}$ with $n=1$, $l=0$ and $n=3$, $l=1$.

With the radial parts given by (3.16), the basis functions $\tilde{\chi}_{Inl}(r)Y_{lm}(\hat{\mathbf{r}})$ are eigenfunctions of hydrogen-like Hamiltonian operator

$$H=-\frac{1}{2}\Delta-\frac{Z_{In}}{r} \tag{3.17}$$

with principle quantum number n. Since in polar coordinates, the normalized bounded eigenfunctions of this operator may be written in the form

$$\varphi_{nlm}(\mathbf{r})=c_{nl}\left(\frac{2Z_{In}r}{n}\right)^l L_{n-l-1}^{2l+1}\left(\frac{2Z_{In}r}{n}\right)\exp\left(-\frac{Z_{In}r}{n}\right)Y_{lm}(\hat{\mathbf{r}}),\quad n-l=1,2,\cdots,$$

we have

$$\tilde{\chi}_{nl}(r)=c_{nl}\left(\frac{2Z_{In}r}{n}\right)^l L_{n-l-1}^{2l+1}\left(\frac{2Z_{In}r}{n}\right)\exp\left(-\frac{Z_{In}r}{n}\right), \tag{3.18}$$

where L_{n-l-1}^{2l+1} is the generalized Laguerre polynomial and c_{nl} is the normalization constant. Note that the eigenfunctions of (3.17) with a fixed Z_{In} do not constitute a complete set, moreover, they spread out quickly and become very diffuse due to the factor $1/n$ in the exponent. This explains why different ionization states have to be taken in (3.13).

One possible choice is to take Z_{In} proportional to the quantum number n. We present in Fig. 3 a comparison of χ_{Inl} and $\tilde{\chi}_{Inl}$ with $Z_{In}=n$, from which we observe that these two types of orbitals are really close to each other as we expected. Therefore, the efficiency of the radial basis functions χ_{Inl} can be illustrated by an error estimates of $\tilde{\chi}_{Inl}$.

Let $Z_{In}=\xi_I n$ with a fixed parameter ξ_I and $\tilde{\chi}_{Inl}$ correspond to principle quantum number n. We have that (3.18) becomes

$$\tilde{\chi}_{Inl}(r)=c_{nl}(2\xi_I r)^l L_{n-l-1}^{2l+1}(2\xi_I r)\exp(-\xi_I r).$$

For simplicity, we will denote ξ_I by ξ afterwards. The finite dimensional space spanned by φ_{nlm} are equivalent to that spanned by STO functions, whose radial parts are products

https://doi.org/10.4208/cicp.170414.231214a Published online by Cambridge University Press

of the monomial r^l and the exponential factor $e^{-\xi r}$

$$\psi_{Inl}(r)=r^{n+l-1}e^{-\xi r},\qquad n=1,2,\cdots. \tag{3.19}$$

To see this, we note that any $\tilde{\chi}_{Inl}(r)$ can be written by linear combination of (3.19) with the power of r between l and $n+l-1$.

The finite dimensional space spanned by STO basis functions (3.19) is

$$V_\delta\equiv V_{NL}=\text{span}\{\psi_{Inl}(r)Y_{lm}(\hat{\mathbf{r}}):\ 1\le I\le M_{\text{n}},\ 1\le n\le N,\ 0\le l\le L,\ |m|\le l\}. \tag{3.20}$$

We have the following estimate for this type of approximations.

Theorem 3.2. *Let V_δ be given by* (3.20). *If u satisfies the assumptions* **A**, **B** *and* **C**, *then for any $s>1$ we have*

$$\inf_{v_\delta\in V_\delta}\|u-v_\delta\|_{H^1(\mathbb{R}^3)}\le C_s(L^{-(s-1)}+N^{-(s-1)/2}+LN^{-s/2})+Ce^{-\alpha R}, \tag{3.21}$$

where C_s is a constant depending on u and s only.

Proof. Using similar arguments as those in the proof of Theorem 3.1, it is only necessary for us to estimate the error of u_I in Ω_I. Let $v_{\delta,I}\in V_\delta$ be spanned by basis functions centered at $\mathbf{R}_I$ (i.e. $v_{\delta,I}(\mathbf{r})=\sum_{n=1}^N\sum_{lm}^L a_{Inlm}\psi_{Inl}(r_I)Y_{lm}(\hat{\mathbf{r}}_I)$), we have

$$\begin{aligned}\|u_I-v_{\delta,I}\|_{H^1(\Omega_I)}\le&\sum_{l=L+1}^{\infty}\sum_{m=-l}^{l}\|u_{Ilm}(r_I)Y_{lm}(\hat{\mathbf{r}}_I)\|_{H^1(\Omega_I)}\\&+\sum_{lm}^{L}\|\big(u_{Ilm}(r_I)-\sum_{n=1}^{N}a_{Inlm}\psi_{Inl}(r_I)\big)Y_{lm}(\hat{\mathbf{r}}_I)\|_{H^1(\Omega_I)},\end{aligned} \tag{3.22}$$

where a_{Inlm}s are coefficients and $u_{Ilm}(r_I)=\int_{S^2}u_I(\mathbf{r}_I)Y_{lm}(\hat{\mathbf{r}}_I)d\hat{\mathbf{r}}_I$. Using standard estimates for spherical harmonics and the assumption **A**, we have

$$\sum_{l=L+1}^{\infty}\sum_{m=-l}^{l}\|u_{Ilm}(r_I)Y_{lm}(\hat{\mathbf{r}}_I)\|_{H^1(\Omega_I)}\le CL^{-(s-1)}\|u_I\|_{H^s([0,R_I^{\text{cut}}]\times S^2)}\quad\forall\, s>1. \tag{3.23}$$

We shall then estimate the second part of the right hand side of (3.22). Let

$$R_{Ilm}(r)=\frac{u_{Ilm}(r)}{r^l}\quad\text{and}\quad v_{\delta,Ilm}(r)=\sum_{n=1}^{N}a_{Inlm}\frac{\psi_{Inl}(r)}{r^l}=\sum_{n=1}^{N}a_{Inlm}r^{n-1}e^{-\xi r}.$$

Note that a simple calculation implies that for $v(r)Y_{lm}(\hat{\mathbf{r}})\in H^1(B(\mathbf{0},R))$,

$$\|v(r)Y_{lm}(\hat{\mathbf{r}})\|^2_{H^1(B(\mathbf{0},R))}=\int_0^R r^2\left(v^2(r)+\left(\frac{\partial v(r)}{\partial r}\right)^2+\frac{l(l+1)}{r^2}v^2(r)\right)dr\int_{S^2}Y_{lm}^2(\hat{\mathbf{r}})d\hat{\mathbf{r}},$$

https://doi.org/10.4208/cicp.170414.231214a Published online by Cambridge University Press

from which we have

$$\begin{aligned}
&\Big\|\big(u_{Ilm}(r_I)-\sum_{n=1}^{N}a_{Inlm}\psi_{Inl}(r_I)\big)Y_{lm}(\hat{\mathbf{r}}_I)\Big\|^2_{H^1(\Omega_I)}\\
=&\|r_I^l(R_{Ilm}(r_I)-v_{\delta,Ilm}(r_I))Y_{lm}(\hat{\mathbf{r}}_I)\|^2_{H^1(\Omega_I)}\\
=&\|r_I^{l+1}(R_{Ilm}(r_I)-v_{\delta,Ilm}(r_I))\|^2_{L^2([0,R_I^{\rm cut}])}+l^2\|r_I^l(R_{Ilm}(r_I)-v_{\delta,Ilm}(r_I))\|^2_{L^2([0,R_I^{\rm cut}])}\\
&+\|r_I^{l+1}\partial_{r_I}(R_{Ilm}(r_I)-v_{\delta,Ilm}(r_I))\|^2_{L^2([0,R_I^{\rm cut}])}\\
&+l(1+l)\|r_I^l(R_{Ilm}(r_I)-v_{\delta,Ilm}(r_I))\|^2_{L^2([0,R_I^{\rm cut}])}\\
\le&\big((R_I^{\rm cut})^2+2l^2+l\big)\|r_I^l(R_{Ilm}(r_I)-v_{\delta,Ilm}(r_I))\|^2_{L^2([0,R_I^{\rm cut}])}\\
&+R_I^{\rm cut}\|r_I^{l+1/2}\partial_{r_I}(R_{Ilm}(r_I)-v_{\delta,Ilm}(r_I))\|^2_{L^2([0,R_I^{\rm cut}])}\\
\lesssim&(1+l^2)\|R_{Ilm}-v_{\delta,Ilm}\|^2_{L^2_{r^{2l}}([0,R_I^{\rm cut}])}+\|\partial_{r_I}(R_{Ilm}-v_{\delta,Ilm})\|^2_{L^2_{r^{2l+1}}([0,R_I^{\rm cut}])}\\
\lesssim&(1+l^2)\|R_{Ilm}-v_{\delta,Ilm}\|^2_{L^2_{r^{2l}}([0,\infty))}+\|\partial_{r_I}(R_{Ilm}-v_{\delta,Ilm})\|^2_{L^2_{r^{2l+1}}([0,\infty))}.
\end{aligned}\tag{3.24}$$

Let $v_{\delta,Ilm}(r)$ be the Laguerre approximation of $R_{Ilm}(r)$ with weight function r^{2l}, that is,

$$v_{\delta,Ilm}(r)=\Pi_{N,r^{2l}}R_{Ilm}(r),$$

where $\Pi_{N,r^{2l}}:L^2_{r^{2l}}([0,\infty))\to\text{span}\{r^{n-1}e^{-\xi r},\,1\le n\le N\}$ is the projection operator defined by

$$(v-\Pi_{N,r^{2l}}v,v_N)_{r^{2l}}=0\quad\forall\,v_N\in\text{span}\{r^{n-1}e^{-\xi r},\,1\le n\le N\}.$$

Using standard spectral approximation results (see [40] for analysis of spectral methods in unbounded domains), we have

$$\begin{aligned}
\|\hat{\partial}^k(R_{Ilm}-\Pi_{N,r^{2l}}R_{Ilm})\|_{L^2_{r^{2l+k}}([0,\infty))}&\le CN^{-(s-k)/2}\|\hat{\partial}^sR_{Ilm}\|_{L^2_{r^{2l+s}}([0,\infty))}\\
&=CN^{-(s-k)/2}\|\hat{\partial}^sR_{Ilm}\|_{L^2_{r^{2l+s}}([0,R_I^{\rm cut}))},
\end{aligned}$$

which together with (3.24) leads to

$$\begin{aligned}
&\Big\|\big(u_{Ilm}(r_I)-\sum_{n=1}^{N}a_{Inlm}\psi_{Inl}(r_I)\big)Y_{lm}(\hat{\mathbf{r}}_I)\Big\|^2_{H^1(\Omega_I)}\\
\le&C(N^{-(s-1)/2}+(1+l)N^{-s/2})\|\hat{\partial}^sR_{Ilm}\|_{L^2_{r^{2l+s}}([0,R_I^{\rm cut}])}.
\end{aligned}\tag{3.25}$$

We obtain from a summation of (3.25) over index l and m that

$$\begin{aligned}
&\sum_{lm}^{L}\Big\|\big(u_{Ilm}(r)-\sum_{n=1}^{N}a_{Inlm}\chi_{Inl}(r)\big)Y_{lm}(\hat{\mathbf{r}})\Big\|_{H^1(\Omega_I)}\\
\le&C(N^{-(s-1)/2}+LN^{-s/2})\left(\sum_{lm}^{L}\|\hat{\partial}^sR_{Ilm}\|_{L^2_{r^{2l+s}}([0,R_I^{\rm cut}])}\right).
\end{aligned}\tag{3.26}$$

https://doi.org/10.4208/cicp.170414.231214a Published online by Cambridge University Press

Taking (3.22), (3.23) and (3.26) into accounts, we have

$$\|u_I - v_{\delta,I}\|_{H^1(\Omega_I)} \leq C_{I,s}(L^{-(s-1)} + N^{-(s-1)/2} + LN^{-s/2}) \tag{3.27}$$

with

$$C_{I,s} = C\left(\|u_I\|_{H^s([0,R_I^{\text{cut}}]\times S^2)} + \sum_{lm}^{L} \|\hat{\partial}^s R_{Ilm}\|_{L^2_{r^{2l+s}}([0,R_I^{\text{cut}}])}\right).$$

By summing up (3.27) over index I and using a similar argument as (3.10), we have from assumption **C** that

$$\|u - v_\delta\|_{H^1(\mathbb{R}^3)} \leq \left(\sum_{I=1}^{M_{\text{n}}} C_{I,s}\right)(L^{-(s-1)} + N^{-(s-1)/2} + LN^{-s/2}) + Ce^{-\alpha R}.$$

Since the assumptions **A** and **B** indicate that $\sum_{I=1}^{M_{\text{n}}} C_{I,s}$ is a finite constant depending only on s and u, we can complete the proof of (3.21). □

Theorem 3.2 gives an a priori error estimate for the STO basis functions under certain reasonable assumptions. We have mentioned that the NAO basis functions with radial parts obtained from (3.13) by taking $Z_{In} = \xi_I n$ are very close to the STO basis functions. Therefore, the super-algebraic convergence rate for STO in (3.21) can illustrate the efficiency of the confined hydrogen-like NAO basis set.

Remark 3.2. This estimate is not strict for the NAO basis functions, but only provides an explanation of the efficiency. In practice, the variational Z_{In}s do not have to be integers, which are usually chosen through an adaptive optimizing procedure such that the basis functions can give the best improvement of a target total energy (see, e.g. [9]). In this case, we shall refer to an a posteriori error estimate of the numerical approximations (see perspectives in Section 5).

4 Numerical experiments

We shall present some numerical experiments in this section to support our theory. All computational results are given by atomic unit (a.u.).

Before showing the numerical results, we want to explain how we perform the numerical integrations, which is one of the most important tasks in NAO based computations. The algorithm we used is based on that in [9, 17, 25], which uses the partitioned integration technique on overlapping, atom-centered grids. In this scheme, each integrand in (3.2) is formally divided into localized atom-centered pieces as

$$H_{ij} = \sum_{I=1}^{M_{\text{n}}} \int_{\Omega_I} p_I(\mathbf{r})\left(\psi_i(\mathbf{r})\hat{h}^{\text{KS}}\psi_j(\mathbf{r})\right)d\mathbf{r}, \tag{4.1}$$

https://doi.org/10.4208/cicp.170414.231214a Published online by Cambridge University Press

where $\hat{h}^{\mathrm{KS}} = -\frac{1}{2}\Delta + v_{\mathrm{eff}}(\mathbf{r})$, and the sum of all atom-centered partition functions $p_I(\mathbf{r})$ equals 1 everywhere, e.g.

$$p_I(\mathbf{r}) = \frac{g_I(\mathbf{r})}{\sum_{I'=1}^{M_{\mathrm{n}}} g_{I'}(\mathbf{r})}$$

with g_I being a strongly peaked function around its originating atom. The Δ operator in $\hat{h}^{\mathrm{KS}}$ include the jump at the spherical surface if the first derivative of the radial basis functions are not continuous at $r = R_I^{\mathrm{cut}}$. The integrand in each atomic sphere is integrated on its own grid of N_r spherical integration shells $r(s)$ $(s = 1, \cdots, N_r)$, on which angular integration points with weights $w_a(t)$ are distributed so as to integrate angular momentums up to a certain accuracy. Specifically, we employ the choice in [9, 17]

$$r(s) = R_I^{\mathrm{cut}} \frac{\log(1-(s/(N_r+1))^2)}{\log(1-(N_r/(N_r+1))^2)}$$

with the radial integration weights $w_r(s)ds = r(s)^2 \frac{dr}{ds}(s)ds$. Also, we shall note that the near-nuclear shells require significantly fewer angular grid points than those outer shells. To sum up, (4.1) is thus given by a summation over integration points

$$H_{ij} = \sum_{I=1}^{M_{\mathrm{n}}} \sum_{s=1}^{N_r} \sum_{t=1}^{N_a} p_I(\mathbf{r}) w_r(s) w_a(t) \big(\psi_i(\mathbf{r}) \hat{h}^{\mathrm{KS}} \psi_j(\mathbf{r})\big). \tag{4.2}$$

Example 1. We first consider the hydrogen (H) atom. We know that the exact ground state energy is -0.5 (a.u.). This is a spherically symmetric system, which only involves $l = 0$ state and is a good example to check the convergence rate on radial basis functions. We show in Fig. 4 the numerical errors of ground state energy approximations by using polynomial-type radial basis set. We observe an exponential convergence rate with respect to the polynomial orders N when N is small. As N increases, the numerical errors decay slower due to the error generated by the cutoff radii. With a larger atomic sphere, the numerical approximations can converge to a more accurate result. We also present the numerical errors by confined hydrogen-like basis functions in Fig. 5. With a sufficient large cutoff radii, the approximations are quite accurate when N is very small. We also observe an exponential convergence rate with respect to the degree of radial basis.

Example 2. We consider the lithium-hydrogen (LiH) molecular. We use a confined hydrogen-like orbital basis set to obtain the ground state approximations, and present the numerical errors with respect to the degrees of radial basis in Fig. 6. The result on the finest discretization is taken to be the exact solution. The numerical errors with respect to the angular numbers are shown in Fig. 7. From these two figures, we observe more or less exponential convergence rates with respect to both N and L, which supports our theory.

https://doi.org/10.4208/cicp.170414.231214a Published online by Cambridge University Press

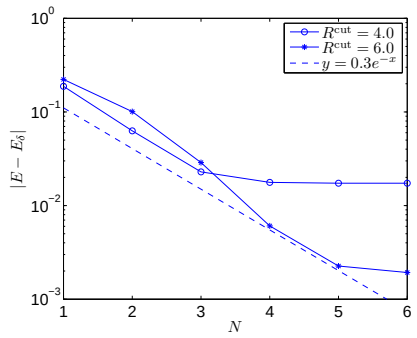


Figure 4: (Example 1) The convergent curve of polynomial-type basis functions.

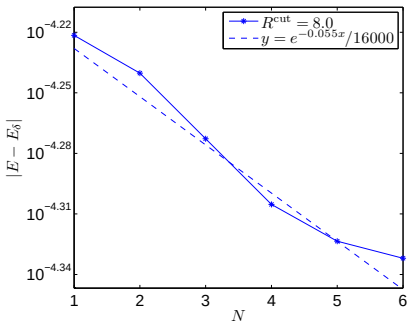


Figure 5: (Example 1) The convergent curve of confined Hydrogen-like basis functions.

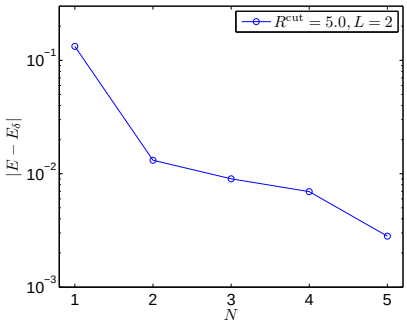


Figure 6: (Example 2) The convergent curve with respect to the degrees of radial basis.

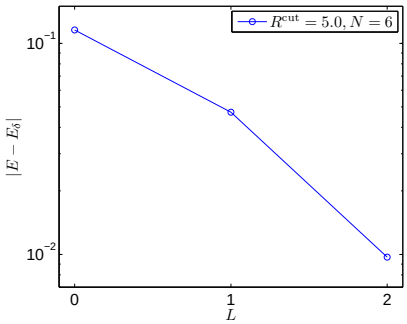


Figure 7: (Example 2) The convergent curve with respect to the angular numbers.

Example 3. We simulate the Fullerene molecular (C60) using the package SIESTA [41]. SIESTA is a computer program to perform efficient electronic structure calculations of molecules and solids, based on KS-DFT and strictly localized basis sets. The atomic configuration of the molecular system is shown in Fig. 8, and we plot an iso-surface of the ground state electron density obtained by SIESTA in Fig. 9. We observe that the iso-surface is actually close to some superposition of atom-centered spheres, as well as some bond formation corresponding to the configuration in Fig. 8 that may be catched by the high angular components. This indicates why atomic orbitals give a good physical descriptions of the electronic states. The convergent curves of ground state energy approximations by SIESTA can be referred to [41].

5 Conclusions and perspectives

In this paper, we present the a priori error estimates for some NAO based approximations in molecular simulations. To our knowledge, this is the first result concerning numerical analysis of NAO basis functions. Although this paper is under KS-DFT framework with

https://doi.org/10.4208/cicp.170414.231214a Published online by Cambridge University Press

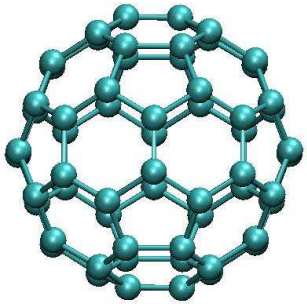


Figure 8: (Example 3) The atomic configuration of the Fullerene molecular.

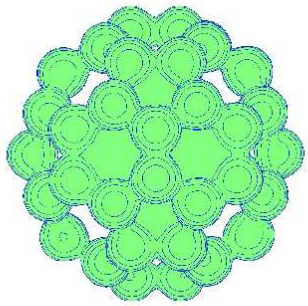


Figure 9: (Example 3) An iso-surface plot of the electron density obtained by SIESTA.

LDA setting, an extension to generalized gradient approximations (GGA), hybrid functionals, Hartree-Fock theory, and MP2/GW formulations for total energies and excited states is possible within the same underlying analysis.

We mention that there are various types of NAO based methods in practical computations, which incorporate the environmental effects by fine tuning the adjustable parameters in the atomic orbitals. The values of the adjustable parameters therefore vary among different chemical elements, exchange-correction potentials, and sometimes ambient environment of atoms, which makes the basis set not transformable and lack of a systematic convergence. For these basis sets, the a priori error estimate can hardly be obtained and the a posteriori analysis is of more interest. The a posteriori analysis provides a more or less precise upper bound of the actual error after a computation has been performed, which may tell you when the desired accuracy is reached and what to do to improve the accuracy. Note that most of the a posteriori analysis are based on relative a priori error estimate. Therefore, our analysis can also be viewed as a preliminary step for further understanding of the NAOs whose effects rely heavily on the experience of the underlying chemical systems.

Acknowledgments

The research for this paper has been enabled by the Alexander von Humboldt Foundation, whose support for the long term visit of Huajie Chen at Technische Universität Berlin is gratefully acknowledged.

References

[1] C.O. Almbladh and U. von Barth, Exact results for the charge and spin densities, exchange-correlation potentials, and density-functional eigenvalues, Phys. Rev. B, 31 (1985), pp. 3231-3244.

[2] S. Agmon, Lectures on the Exponential Decay of Solutions of Second-Order Elliptic Operators, Princeton University Press, Princeton, 1981.

https://doi.org/10.4208/cicp.170414.231214a Published online by Cambridge University Press

[3] A. Anantharaman and E. Cancès, Existence of minimizers for Kohn-Sham models in quantum chemistry, Ann. I. H. Poincaré-AN, 26 (2009), pp. 2425-2455.
[4] F.W. Averill and D.E. Ellis, An efficient numerical multicenter basis set for molecular orbital calculations: application to FeCl4 J. Chem. Phys., 59 (1973), pp. 6412-6418.
[5] M. Bachmayr, H. Chen, and R. Schneider, Error estimates for Hermite and even-tempered Gaussian approximations in quantum chemistry, Numer. Math., 128 (2014), pp. 137-165.
[6] I. Babuška and M. Rosenzweig, A finite element scheme for domains with corners, Numer. Math., 20 (1972), pp. 1-21.
[7] D. Braess, Asymptotics for the approximation of wave functions by sums of exponentials, J. Approximation Theory, 83 (1995), pp. 93-103.
[8] D. Braess and W. Hackbusch, Approximation of $1/x$ by exponential sums in $[1,\infty)$, IMA J. Numer. Anal., 25 (2005), pp. 685-697.
[9] V. Blum, R. Gehrke, F. Hanke, P. Havu, V. Havu, X. Ren, K. Reuter, Ab initio molecular simulations with numeric atom-centered orbitals, Comp. Phys. Commun., bf 180 (2009), pp. 2175-2196.
[10] S.F. Boys, Electron wave functions I. A general method for calculation for the stationary states of any molecular system, Proc. Roy. Soc. London, series A, 200 (1950), pp. 542-554.
[11] P. Grisvard, Singularities in boundary value problems, volume 22 of Research in Applied Mathematics, Masson, Paris, 1992.
[12] E. Cancès, R. Chakir, and Y. Maday, Numerical analysis of the planewave discretization of some orbital-free and Kohn-Sham models, M2AN, 46 (2012), pp. 341-388.
[13] C. Canuto, M.Y. Hussaini, A. Quarteroni, T.A. Zang, Spectral Methods for Fluid Dynamics, Springer-Verlag, 1988.
[14] H. Chen, X. Gong, L. He, Z. Yang, and A. Zhou, Numerical analysis of finite dimensional approximations of Kohn-Sham models, Adv. Comput. Math., 38 (2013), pp 225-256.
[15] H. Chen and R. Schneider, Numerical analysis of augmented plane waves methods for full-potential electronic structure calculations, M2AN, DOI: http://dx.doi.org/10.1051/m2an/2014052.
[16] P.G. Ciarlet ed., Handbook of Numerical Analysis, Vol. II. Finte Element Methods, North-Holland, Amsterdam, 1990.
[17] B. Delley, An all-electron numerical method for solving the local density functional for polyatomic molecules, J. Chem. Phys., 92 (1990), pp. 508-517.
[18] Y.V. Egorov and B.W. Schulze, Pseudo-differential Operators, Singularities, Applications, Birkhäuse, Basel, 1997.
[19] H.J. Flad, R. Schneider, and B.W. Schulze, Asymptotic regularity of solutions to Hartree-Fock equations with Coulomb potential, Math. Meth. Appl. Sci., 31 (2008), pp. 2172-2201.
[20] S. Fournais, M. Hoffmann-Ostenhof, T. Hoffmann-Ostenhof, and T. Østergaard Sørensen, The electron density is smooth away from the nuclei, Communications in Mathematical Physics, 228 (2002), pp. 401-415.
[21] S. Fournais, M. Hoffmann-Ostenhof, T. Hoffmann-Ostenhof, and T. Østergaard Sørensen, Analyticity of the density of electronic wavefunctions, Arkiv för Matematik, 42 (2004), pp. 87-106.
[22] S. Fournais, M. Hoffmann-Ostenhof, T. Hoffmann-Ostenhof, and T. Østergaard Sørensen, Non-isotropic cusp conditions and regularity of the electron density of molecules at the nuclei, Annales Henri Poincaré, 8 (2007), pp. 731-748.
[23] S. Goedecker and L. Colombo, Efficient linear scaling algorithm for tight binding molecular dynamics, Phys. Rev. Lett., 73 (1994), pp. 122-125.

https://doi.org/10.4208/cicp.170414.231214a Published online by Cambridge University Press

[24] X. Gong, L. Shen, D. Zhang, and A. Zhou, Finite element approximations for Schrödinger equations with applications to electronic structure computations, J. Comput. Math., 23 (2008), pp. 310-327.
[25] V. Havu, V. Blum, P. Havu, M. Scheffler, Efficient O(N) integration for all-electron electronic structure calculation using numeric basis functions, J. Comput. Phys., 228 (2009), pp. 8367-8379.
[26] M. Hoffmann-Ostenhof, T. Hoffmann-Ostenhof, and T. Østergaard Sørensen, Electron wavefunctions and densities for atoms, Annales Henri Poincaré, 2 (2001), pp. 77-100.
[27] T. Helgaker, P. Jorgensen, and J. Olsen, Molecular Electronic-Structure Theory, Wiley, 2000.
[28] P. Hohenberg and W. Kohn, Inhomogeneous Electron Gas, Phys. Rev. B, 136 (1964), pp. 864-871.
[29] J. Junquera, O. Paz, D. Sanchez-Portal, and E. Artacho, Numerical atomic orbitals for linear-scaling calculations, Phys. Rev. B, 64 (2001), pp. 235111-1-23.
[30] W. Kohn and L.J. Sham, Self-consistent equations including exchange and correlation effects, Phys. Rev. A, 140 (1965), pp. 1133-1138.
[31] W. Kutzelnigg, Theory of the expansion of wave functions in a Gaussian Basis, Int. J. Quantum Chem., 51 (1994), pp. 447-463.
[32] W. Kutzelnigg, Convergence of expansions in a Gaussian basis, in Strategies and Applications in Quantum Chemistry Topics in Molecular Organization and Engineering, Volume 14, 2 (2002), pp. 79-101.
[33] C. Le Bris, ed., Handbook of Numerical Analysis, Vol. X. Special issue: Computational Chemistry, North-Holland, Amsterdam, 2003.
[34] E.H. Lieb and B. Simon, The Hartree-Fock theory for Coulomb systems, Comm. Math. Phys., 53 (1977), pp. 185-194.
[35] G. Lippert, J. Hutter, P. Ballone, and M. Parrinello, Response function basis sets: Application to density functional calculations, J. Phys. Chem., 100 (1996), pp. 6231-6235.
[36] R.M. Martin, Electronic Structure: Basic Theory and Practical Methods, Cambridge University Press, 2005.
[37] R.D. McWeeny and B.T. Sutcliffe, Methods of Molecular Quantum Mechanics, second edition, Academic Press, New York, 1976.
[38] J.E. Osborn, Spectral approximation for compact operators, Mathematics of Computation, 29 (1975), pp. 712-725.
[39] T. Ozaki and H. Kino, Numerical atomic basis orbitals from H to Kr, Phys. Rev. B 69 (2004), pp. 195113-1-19.
[40] J. Shen and L. Wang, Some recent advances on spectral methods for unbounded domains, Commun. Comput. Phys., 5 (2009), pp. 195-241.
[41] J.M Soler, E. Artacho, J.D. Gale, A. García, J. Junquera, P. Ordejón, and D. Sánchez-Portal, The SIESTA method for ab initio order-N materials simulation, J. Phys. Condens. Matter, 14 (2002), pp. 2745-2779.
[42] A. Szabo and N.S. Ostlund, Modern Quantum Chemistry: Introduction to Advanced Electronic Structure Theory, Dover, Mineola, New York, 1996.
[43] H. Yserentant, Regularity and Approximability of Electronic Wave Functions, Springer Heidelberg Dordrech London New York, 2000.
[44] A. Zunger and A.J. Freeman, Self-consistent numerical-basis-set linear-combination-of-atomic-orbitals model for the study of solids in the local density formalism, Phys. Rev. B, 15 (1977), pp. 4716-4737.

https://doi.org/10.4208/cicp.170414.231214a Published online by Cambridge University Press